



A study of single and multi-photon production in e^+e^- collisions at centre-of mass energies of 130 and 136 GeV

D. Buskalic, I. De Bonis, D. Decamp, P. Ghez, C. Goy, J.P. Lees, A. Lucotte, M.N. Minard, P. Odier, B. Pietrzyk, et al.

► To cite this version:

D. Buskalic, I. De Bonis, D. Decamp, P. Ghez, C. Goy, et al.. A study of single and multi-photon production in e^+e^- collisions at centre-of mass energies of 130 and 136 GeV. Physics Letters B, Elsevier, 1996, 384, pp.333-342. <in2p3-00011566>

HAL Id: in2p3-00011566

<http://hal.in2p3.fr/in2p3-00011566>

Submitted on 18 Mar 1999

HAL is a multi-disciplinary open access archive for the deposit and dissemination of scientific research documents, whether they are published or not. The documents may come from teaching and research institutions in France or abroad, or from public or private research centers.

L'archive ouverte pluridisciplinaire **HAL**, est destinée au dépôt et à la diffusion de documents scientifiques de niveau recherche, publiés ou non, émanant des établissements d'enseignement et de recherche français ou étrangers, des laboratoires publics ou privés.

A study of single and multi-photon production in $e^+ e^-$ collisions at centre-of-mass energies of 130 and 136 GeV

The ALEPH Collaboration

Abstract

The production of final states involving one or more energetic photons from e^+e^- collisions at high energies is studied using data collected by the ALEPH detector at LEP. The data consist of two samples of 2.9 pb^{-1} each, recorded at centre-of-mass energies of 130 GeV and 136 GeV. The data are in agreement with the predictions of the Standard Model. From an analysis of two-photon final states new limits are placed on the parameters of models involving $e^+e^-\gamma\gamma$ contact interactions and excited electrons. The 95% confidence level lower limits on the QED cut-off parameters Λ_+ and Λ_- are found to be 169 and 132 GeV respectively.

(Submitted to Physics Letters B)

The ALEPH Collaboration

D. Buskalic, I. De Bonis, D. Decamp, P. Ghez, C. Goy, J.-P. Lees, A. Lucotte, M.-N. Minard, P. Odier, B. Pietrzyk

Laboratoire de Physique des Particules (LAPP), IN²P³-CNRS, 74019 Annecy-le-Vieux Cedex, France

M.P. Casado, M. Chmeissani, J.M. Crespo, M. Delfino,¹² I. Efthymiopoulos,²⁰ E. Fernandez, M. Fernandez-Bosman, Ll. Garrido,¹⁵ A. Juste, M. Martinez, S. Orteu, C. Padilla, A. Pascual, J.A. Perlas, I. Riu, F. Sanchez, F. Teubert
Institut de Fisica d'Altes Energies, Universitat Autònoma de Barcelona, 08193 Bellaterra (Barcelona), Spain⁷

A. Colaleo, D. Creanza, M. de Palma, G. Gelao, M. Girone, G. Iaselli, G. Maggi,³ M. Maggi, N. Marinelli, S. Nuzzo, A. Ranieri, G. Raso, F. Ruggieri, G. Selvaggi, L. Silvestris, P. Tempesta, G. Zito
Dipartimento di Fisica, INFN Sezione di Bari, 70126 Bari, Italy

X. Huang, J. Lin, Q. Ouyang, T. Wang, Y. Xie, R. Xu, S. Xue, J. Zhang, L. Zhang, W. Zhao
Institute of High-Energy Physics, Academia Sinica, Beijing, The People's Republic of China⁸

R. Alemany, A.O. Bazarko, M. Cattaneo, P. Comas, P. Coyle, H. Drevermann, R.W. Forty, M. Frank, R. Hagelberg, J. Harvey, P. Janot, B. Jost, E. Kneringer, J. Knobloch, I. Lehraus, G. Lutters, E.B. Martin, P. Mato, A. Minten, R. Miquel, Ll.M. Mir,² L. Moneta, T. Oest,¹ A. Pacheco, J.-F. Puztaszeri, F. Ranjard, P. Rensing,²⁵ L. Rolandi, D. Schlatter, M. Schmelling,²⁴ O. Schneider, W. Tejessy, I.R. Tomalin, A. Venturi, H. Wachsmuth, A. Wagner
European Laboratory for Particle Physics (CERN), 1211 Geneva 23, Switzerland

Z. Ajaltouni, A. Barrès, C. Boyer, A. Falvard, P. Gay, C. Guicheney, P. Henrard, J. Jousset, B. Michel, S. Monteil, J.-C. Montret, D. Pallin, P. Perret, F. Podlyski, J. Proriot, P. Rosnet, J.-M. Rossignol
Laboratoire de Physique Corpusculaire, Université Blaise Pascal, IN²P³-CNRS, Clermont-Ferrand, 63177 Aubière, France

T. Fearnley, J.B. Hansen, J.D. Hansen, J.R. Hansen, P.H. Hansen, B.S. Nilsson, A. Wäänänen
Niels Bohr Institute, 2100 Copenhagen, Denmark⁹

A. Kyriakis, C. Markou, E. Simopoulou, I. Siotis, A. Vayaki, K. Zachariadou
Nuclear Research Center Demokritos (NRCD), Athens, Greece

A. Blondel, J.C. Brient, A. Rougé, M. Rumpf, A. Valassi,⁶ H. Videau²¹
Laboratoire de Physique Nucléaire et des Hautes Energies, Ecole Polytechnique, IN²P³-CNRS, 91128 Palaiseau Cedex, France

E. Focardi,²¹ G. Parrini
Dipartimento di Fisica, Università di Firenze, INFN Sezione di Firenze, 50125 Firenze, Italy

M. Corden, C. Georgiopoulos, D.E. Jaffe
Supercomputer Computations Research Institute, Florida State University, Tallahassee, FL 32306-4052, USA^{13,14}

A. Antonelli, G. Bencivenni, G. Bologna,⁴ F. Bossi, P. Campana, G. Capon, D. Casper, V. Chiarella, G. Felici, P. Laurelli, G. Mannocchi,⁵ F. Murtas, G.P. Murtas, L. Passalacqua, M. Pepe-Altarelli
Laboratori Nazionali dell'INFN (LNF-INFN), 00044 Frascati, Italy

L. Curtis, S.J. Dorris, A.W. Halley, I.G. Knowles, J.G. Lynch, V. O'Shea, C. Raine, P. Reeves, J.M. Scarr, K. Smith, A.S. Thompson, F. Thomson, S. Thorn, R.M. Turnbull
Department of Physics and Astronomy, University of Glasgow, Glasgow G12 8QQ, United Kingdom¹⁰

U. Becker, C. Geweniger, G. Graefe, P. Hanke, G. Hansper, V. Hepp, E.E. Kluge, A. Putzer, B. Rensch, M. Schmidt, J. Sommer, H. Stenzel, K. Tittel, S. Werner, M. Wunsch
Institut für Hochenergiephysik, Universität Heidelberg, 69120 Heidelberg, Fed. Rep. of Germany¹⁶

D. Abbaneo, R. Beuselinck, D.M. Binnie, W. Cameron, P.J. Dornan, A. Moutoussi, J. Nash, J.K. Sedgbeer, A.M. Stacey, M.D. Williams

Department of Physics, Imperial College, London SW7 2BZ, United Kingdom¹⁰

G. Dissertori, P. Girtler, D. Kuhn, G. Rudolph

Institut für Experimentalphysik, Universität Innsbruck, 6020 Innsbruck, Austria¹⁸

A.P. Betteridge, C.K. Bowdery, P. Colrain, G. Crawford, A.J. Finch, F. Foster, G. Hughes, T. Sloan, E.P. Whelan, M.I. Williams

Department of Physics, University of Lancaster, Lancaster LA1 4YB, United Kingdom¹⁰

A. Galla, A.M. Greene, C. Hoffmann, K. Kleinknecht, G. Quast, B. Renk, E. Rohne, H.-G. Sander, P. van Gemmeren C. Zeitnitz

Institut für Physik, Universität Mainz, 55099 Mainz, Fed. Rep. of Germany¹⁶

J.J. Aubert,²¹ A.M. Bencheikh, C. Benchouk, A. Bonissent,²¹ G. Bujosa, D. Calvet, J. Carr, C. Diaconu, N. Konstantinidis, P. Payre, D. Rousseau, M. Talby, A. Sadouki, M. Thulasidas, A. Tilquin, K. Trabelsi

Centre de Physique des Particules, Faculté des Sciences de Luminy, IN²P³-CNRS, 13288 Marseille, France

M. Aleppo, F. Ragusa²¹

Dipartimento di Fisica, Università di Milano e INFN Sezione di Milano, 20133 Milano, Italy.

I. Abt, R. Assmann, C. Bauer, W. Blum, H. Dietl, F. Dydak,²¹ G. Ganis, C. Gotzhein, K. Jakobs, H. Kroha, G. Lütjens, G. Lutz, W. Männer, H.-G. Moser, R. Richter, A. Rosado-Schlosser, S. Schael, R. Settles, H. Seywerd, R. St. Denis, W. Wiedenmann, G. Wolf

Max-Planck-Institut für Physik, Werner-Heisenberg-Institut, 80805 München, Fed. Rep. of Germany¹⁶

J. Boucrot, O. Callot, A. Cordier, M. Davier, L. Duflot, J.-F. Grivaz, Ph. Heusse, A. Höcker, M. Jacquet, D.W. Kim,¹⁹ F. Le Diberder, J. Lefrançois, A.-M. Lutz, I. Nikolic, H.J. Park,¹⁹ I.C. Park,¹⁹ M.-H. Schune, S. Simion, J.-J. Veillet, I. Videau, D. Zerwas

Laboratoire de l'Accélérateur Linéaire, Université de Paris-Sud, IN²P³-CNRS, 91405 Orsay Cedex, France

P. Azzurri, G. Bagliesi, G. Batignani, S. Bettarini, C. Bozzi, G. Calderini, M. Carpinelli, M.A. Ciocci, V. Ciulli, R. Dell'Orso, R. Fantechi, I. Ferrante, A. Giassi, A. Gregorio, F. Ligabue, A. Lusiani, P.S. Marrocchesi, A. Messineo, F. Palla, G. Rizzo, G. Sanguinetti, A. Sciabà, P. Spagnolo, J. Steinberger, R. Tenchini, G. Tonelli,²⁶ C. Vannini, P.G. Verdini, J. Walsh

Dipartimento di Fisica dell'Università, INFN Sezione di Pisa, e Scuola Normale Superiore, 56010 Pisa, Italy

G.A. Blair, L.M. Bryant, F. Cerutti, J.T. Chambers, Y. Gao, M.G. Green, T. Medcalf, P. Perrodo, J.A. Strong, J.H. von Wimmersperg-Toeller

Department of Physics, Royal Holloway & Bedford New College, University of London, Surrey TW20 OEX, United Kingdom¹⁰

D.R. Botterill, R.W. Clift, T.R. Edgecock, S. Haywood, P. Maley, P.R. Norton, J.C. Thompson, A.E. Wright
Particle Physics Dept., Rutherford Appleton Laboratory, Chilton, Didcot, Oxon OX11 0QX, United Kingdom¹⁰

B. Bloch-Devau, P. Colas, S. Emery, W. Kozanecki, E. Lançon, M.C. Lemaire, E. Locci, B. Marx, P. Perez, J. Rander, J.-F. Renardy, A. Roussarie, J.-P. Schuller, J. Schwindling, A. Trabelsi, B. Vallage

CEA, DAPNIA/Service de Physique des Particules, CE-Saclay, 91191 Gif-sur-Yvette Cedex, France¹⁷

S.N. Black, J.H. Dann, R.P. Johnson, H.Y. Kim, A.M. Litke, M.A. McNeil, G. Taylor

Institute for Particle Physics, University of California at Santa Cruz, Santa Cruz, CA 95064, USA²²

C.N. Booth, R. Boswell, C.A.J. Brew, S. Cartwright, F. Combley, A. Koksai, M. Letho, W.M. Newton, J. Reeve, L.F. Thompson

Department of Physics, University of Sheffield, Sheffield S3 7RH, United Kingdom¹⁰

A. Böhrer, S. Brandt, V. Büscher, G. Cowan, C. Grupen, P. Saraiva, L. Smolik, F. Stephan,
*Fachbereich Physik, Universität Siegen, 57068 Siegen, Fed. Rep. of Germany*¹⁶

M. Apollonio, L. Bosisio, R. Della Marina, G. Giannini, B. Gobbo, G. Musolino
Dipartimento di Fisica, Università di Trieste e INFN Sezione di Trieste, 34127 Trieste, Italy

J. Putz, J. Rothberg, S. Wasserbaech, R.W. Williams
Experimental Elementary Particle Physics, University of Washington, WA 98195 Seattle, U.S.A.

S.R. Armstrong, L. Bellantoni,²³ P. Elmer, Z. Feng,²⁸ D.P.S. Ferguson, Y.S. Gao,²⁹ S. González, J. Grahl,
T.C. Greening, O.J. Hayes, H. Hu, P.A. McNamara III, J.M. Nachtman, W. Orejudos, Y.B. Pan, Y. Saadi,
M. Schmitt, I.J. Scott, A.M. Walsh,²⁷ Sau Lan Wu, X. Wu, J.M. Yamartino, M. Zheng, G. Zoernig
*Department of Physics, University of Wisconsin, Madison, WI 53706, USA*¹¹

¹Now at DESY, Hamburg, Germany.

²Supported by Dirección General de Investigación Científica y Técnica, Spain.

³Now at Dipartimento di Fisica, Università di Lecce, 73100 Lecce, Italy.

⁴Also Istituto di Fisica Generale, Università di Torino, Torino, Italy.

⁵Also Istituto di Cosmo-Geofisica del C.N.R., Torino, Italy.

⁶Supported by the Commission of the European Communities, contract ERBCHBICT941234.

⁷Supported by CICYT, Spain.

⁸Supported by the National Science Foundation of China.

⁹Supported by the Danish Natural Science Research Council.

¹⁰Supported by the UK Particle Physics and Astronomy Research Council.

¹¹Supported by the US Department of Energy, grant DE-FG0295-ER40896.

¹²Also at Supercomputations Research Institute, Florida State University, Tallahassee, U.S.A.

¹³Supported by the US Department of Energy, contract DE-FG05-92ER40742.

¹⁴Supported by the US Department of Energy, contract DE-FC05-85ER250000.

¹⁵Permanent address: Universitat de Barcelona, 08208 Barcelona, Spain.

¹⁶Supported by the Bundesministerium für Forschung und Technologie, Fed. Rep. of Germany.

¹⁷Supported by the Direction des Sciences de la Matière, C.E.A.

¹⁸Supported by Fonds zur Förderung der wissenschaftlichen Forschung, Austria.

¹⁹Permanent address: Kangnung National University, Kangnung, Korea.

²⁰Now at CERN, 1211 Geneva 23, Switzerland.

²¹Also at CERN, 1211 Geneva 23, Switzerland.

²²Supported by the US Department of Energy, grant DE-FG03-92ER40689.

²³Now at Fermi National Accelerator Laboratory, Batavia, IL 60510, USA.

²⁴Now at Max-Planck-Institut für Kernphysik, Heidelberg, Germany.

²⁵Now at Dragon Systems, Newton, MA 02160, U.S.A.

²⁶Also at Istituto di Matematica e Fisica, Università di Sassari, Sassari, Italy.

²⁷Now at Rutgers University, Piscataway, NJ 08855-0849, U.S.A.

²⁸Now at The Johns Hopkins University, Baltimore, MD 21218, U.S.A.

²⁹Now at Harvard University, Cambridge, MA 02138, U.S.A.

1 Introduction

The annihilation of electrons and positrons into final states in which the only observable particles are energetic photons is well understood within the framework of the Standard Model. Such final states are therefore well suited to the search for new physics. Events with a single isolated photon are expected to be produced predominantly via initial state radiation accompanied by the production of a Z boson, which subsequently decays via $Z \rightarrow \nu\bar{\nu}$. Such events together with new physics processes which would give rise to energetic single photons [1, 2] have been studied at energies around the Z peak [3] and around 130 GeV [4, 5]. Events with two (or more) energetic photons are expected to be produced via t channel electron exchange. Previous studies of these events, at centre-of-mass energies around the Z peak [6, 7, 8] and around 130 GeV [5, 9], have found results in agreement with the predictions of QED. Deviations from the expected QED differential cross section for the production of two photons could be evidence for new physics due to, for example, $e^+e^-\gamma\gamma$ “contact interactions” [8, 10, 11] or excited electrons.

This letter is based on data collected in a short run of LEP in 1995 at centre-of-mass energies of 130 and 136 GeV. Although the integrated luminosity is rather limited (2.9 pb^{-1} at each energy) it is worthwhile examining the data sample for deviations from QED as this is the first opportunity to study e^+e^- collisions at centre-of-mass energies significantly above the Z mass. Also, limits on cut-off parameters for contact interactions improve with the centre-of-mass energy to the power three-quarters but only with the eighth root of the integrated luminosity.

2 The ALEPH detector and photon identification

The ALEPH detector is described in detail elsewhere [12]. The analysis presented here depends largely on the performance of the electromagnetic calorimeter (ECAL). The luminosity calorimeters (LCAL and SICAL), together with the hadron calorimeter (HCAL), were used mainly to veto events where photons are accompanied by other energetic particles. The tracking system, composed of a silicon vertex detector, wire drift chamber, and time projection chamber, was used to provide efficient ($> 99.9\%$) tracking of charged particles in the angular range $|\cos\theta| < 0.96$.

The ECAL is a lead/wire-plane sampling calorimeter. It consists of 36 modules, twelve in the barrel and twelve in each endcap, which provide coverage in the angular range $|\cos\theta| < 0.98$. Inter-module gaps reduce this solid angle coverage by 2% in the barrel and 6% in the endcaps. The total thickness of the ECAL is 22 radiation lengths at normal incidence. The longitudinal sampling consists of 45 layers of lead, 2 mm thick in the first 13 radiation lengths (33 layers) and 4 mm thick in the remainder (12 layers). Anode wire signals, sampled every 512 ns during their rise time, provide a measurement by the ECAL of the interaction time t_0 of the particles relative to the beam crossing with a resolution better than 15 ns. Cathode pads associated with each layer of the wire chambers are connected to form projective “towers”, each subtending approximately $0.9^\circ \times 0.9^\circ$, which are oriented towards the interaction point. Each tower is read out in three segments in depth of four, nine and nine radiation lengths. The high granularity of the calorimeter provides for excellent identification of photons and electrons. The energy calibration of each module is determined from Bhabha events. The energy resolution is measured to be $\Delta E/E = 0.18/\sqrt{E} + 0.009$ (E in GeV) [13].

Photon candidates were identified using an algorithm [13] which performs a topological search for localised energy depositions within clusters (groups of neighboring ECAL towers with significant energy deposition). These localised energy depositions are required to have a transverse

and longitudinal profile consistent with that of an electromagnetic shower. Photon candidates may also be identified if they convert producing an electron-positron pair. Only one such converted photon was allowed per event. Furthermore, events which had charged tracks not associated with an identified pair conversion were rejected. All photon candidates were required to have an energy above 1 GeV and lie within an angular acceptance of $|\cos\theta| < 0.95$. Cosmic ray background together with detector noise (sparks and radioactive decays inside the calorimeter materials) were further suppressed by requiring that the interaction time t_0 of the event be within 120 ns of the beam crossing.

The trigger for events with isolated photons is based exclusively on the energy measured using the wire planes of the ECAL. The efficiency of this trigger has been studied with a sample of hadronic events obtained using an independent trigger. For energies above 10 GeV this trigger has been found to be essentially 100% efficient. For this analysis the LCAL was used to provide the luminosity measurement.

3 The process $e^+e^- \rightarrow \nu\bar{\nu}\gamma(\gamma)$

Events where photons are produced accompanied by purely weakly interacting particles were selected according to the following criteria. Each event was required to have at least one photon candidate with an energy above 10 GeV. To suppress cosmic ray background, further cuts were applied to this tagging photon. The fraction of the ECAL cluster energy reconstructed in the four towers nearest the cluster barycentre was required to be at least 0.7. The energy fractions in the first and second segments in depth must be less than 0.5 and 0.9 respectively. Backgrounds coming from cosmic rays and beam related muons were also rejected by removing events with a penetrating pattern in the HCAL/muon chambers. Radiative Bhabha events were rejected by requiring that there be no energy deposition in the event above 1 GeV which was not associated with a photon candidate. The component of radiative Bhabha scattering where both the electron and positron escape detection in the beam pipe was excluded by the effective transverse momentum cut on the tagging photon of 3.2 GeV/c combined with the SICAL acceptance (down to 24.3 mrad from the beam axis). Events with two or more photons coming from the process $e^+e^- \rightarrow \gamma\gamma(\gamma)$ were removed as follows. Events with only two photons were required to have an acoplanarity of at most 170°. Events with three or more photons were simply required to have at least 30 GeV of missing energy.

The efficiency of the above selection criteria to select signal events with a single photon inside the acceptance is estimated to be $85 \pm 1\%$. The inefficiency arose mainly from the effect of the inter-module gaps (5%) and the additional photon selection criteria applied to the tagging photon (4%). The remaining sources of inefficiencies were due to non-identified photon conversions (2%) and the presence of additional photons, from the signal process, inside the acceptance (4%). This estimation was obtained from a sample of events produced by the NUNUGG [14] Monte Carlo generator which were subsequently passed through the full ALEPH simulation and reconstruction programs. This generator gives a full treatment of hard photon emission to order α^2 with exponentiation of the soft photon spectra. When the above selection criteria were applied to the data sample, a total of 40 single-photon candidates were obtained: 23 from the 130 GeV data sample and 17 from the 136 GeV data sample. No two-photon candidates were observed compared with a Monte Carlo prediction of 2 events. No events were observed with three or more photon candidates.

The invariant mass distribution of the system recoiling against the photon candidate, as shown

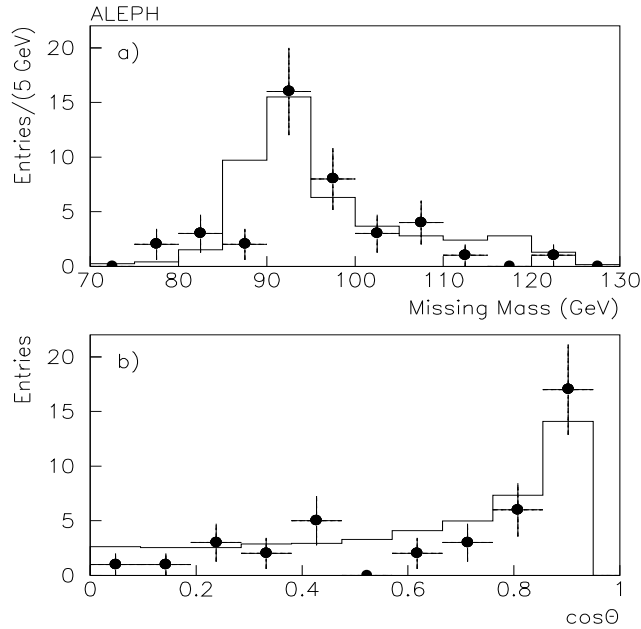


Figure 1: a) The invariant mass distribution of the system recoiling against the photon candidate is shown for both data (with error bars) and Monte Carlo simulation (histogram). b) The corresponding plot of the polar angle distribution of the photon candidate.

in Fig. 1a, clusters around the Z boson mass as expected from the Monte Carlo simulation. The polar angle distribution of the selected events, shown in Fig. 1b, is also seen to agree with the Standard Model prediction. In both figures the data from the 130 GeV and 136 GeV data samples are shown together and are compared to suitably normalised samples of 130 GeV and 136 GeV Monte Carlo.

The observed numbers of single-photon events were used to derive measurements of the cross sections for the process $e^+e^- \rightarrow \nu\bar{\nu}\gamma(\gamma)$ inside the acceptance $E > 10$ GeV, $|\cos\theta| < 0.95$:

$$\sigma(e^+e^- \rightarrow \nu\bar{\nu}\gamma(\gamma)) = 9.6 \pm 2.0(stat.) \pm 0.3(syst.) \text{ pb at 130 GeV}$$

and

$$\sigma(e^+e^- \rightarrow \nu\bar{\nu}\gamma(\gamma)) = 7.2 \pm 1.7(stat.) \pm 0.2(syst.) \text{ pb at 136 GeV.}$$

These results are consistent with the Standard Model predictions, obtained using the NUNUGG generator, of 10.7 ± 0.2 pb at 130 GeV and 9.1 ± 0.2 pb at 136 GeV.

The estimates of the systematic uncertainties in the above cross sections include contributions from the sources listed in Table 1. The ability of the Monte Carlo to simulate the selection efficiency for energetic photons accurately was checked with a sample of Bhabha events selected using only tracking and muon chamber information. The tracking information was masked from these events and the photon reconstruction redone. The efficiency to select a single “photon” in these events was found to be consistent between data and Monte Carlo simulation at the 1% level. The uncertainty in the number of simulated pair conversions is estimated to give a 0.3% change

| | |
|----------------------------|--------|
| Photon selection | 1.0% |
| Converted photon selection | 0.3% |
| Residual cosmic background | 1.8% |
| Random vetoing | 0.5% |
| Integrated luminosity | 0.9% |
| Monte Carlo theoretical | < 1.0% |
| Monte Carlo statistical | 2.0% |
| Total (in quadrature) | 2.9% |

Table 1: Systematic uncertainties in the single-photon analysis.

in the overall efficiency. An estimate of the background contribution coming from cosmic rays and detector noise was obtained by selecting events slightly out of time with respect to the beam crossing but which passed all other cuts. A total of two such events were observed inside a timing window $120 \text{ ns} < |t_0| < 480 \text{ ns}$, which corresponds to an expectation of 0.7 ± 0.5 events in the selected data sample. An additional inefficiency caused by detector and beam related noise was measured from a sample of random triggers to be $2.3 \pm 0.3\%$. The cross sections quoted above are corrected to take this effect into account. An uncertainty of 0.5% is assigned to this correction since the rate of the random triggers did not follow the variations in luminosity observed during data taking. A second independent Monte Carlo generator KORALZ [15], which produces an arbitrary number of hard photons via exponentiation, gave a consistent (better than 1%) prediction for the cross section.

4 The process $e^+e^- \rightarrow \gamma\gamma(\gamma)$

4.1 Event selection

Each event was required to have at least two identified photons with an energy above $0.22 \times \sqrt{s}$. The angle between the two most energetic photons was required to be greater than 120° . The above cuts resulted in the selection of 81 events, of which 10 contain a converted photon candidate. The corresponding QED expectation based on the multi-photon generator GGG [16] is 102 events, of which 8 are expected in the converted photon sample. The efficiency of the above selection criteria, for events generated inside the angular range $|\cos\theta| < 0.95$, was determined from the above Monte Carlo sample to be 85%.

Within the selected sample, four events were found to have a third photon inside the angular acceptance with an energy of at least 1 GeV and separated from the first two photons by at least 8° , consistent with the Monte Carlo expectation of 5.5 events. The properties of these three-photon events were studied and found to be consistent with Monte Carlo expectations. No events were found in the data sample with four photons inside the acceptance, consistent with an expectation of 0.3 events based on a Monte Carlo simulation using an order α^4 generator FGAM [17].

The only significant background to the photonic final state process is Bhabha scattering accompanied by hard initial state radiation. Monte Carlo simulation of this process [18] shows that only one such background event is expected in the data sample.

The lowest order Born cross section for electron-positron annihilation into two photons is given

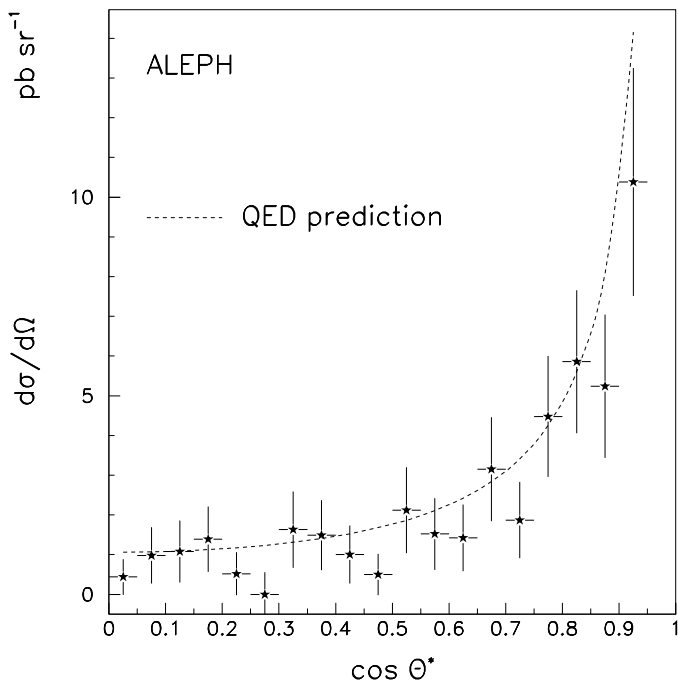


Figure 2: Predicted and observed lowest-order differential cross section as a function of $\cos \theta^*$ for the reaction $e^+e^- \rightarrow \gamma\gamma$. The errors shown here are purely statistical.

by

$$\left(\frac{d\sigma}{d\Omega}\right)_{\text{Born}} = \frac{\alpha^2}{s} \left(\frac{1 + \cos^2 \theta}{1 - \cos^2 \theta}\right),$$

where θ is the angle of a photon with respect to the positron direction. The observed cross section is modified by two effects; higher order processes, in particular initial state radiation, and detector effects. Due to initial state radiation, the centre-of-mass frame of the two detected photons is not necessarily at rest in the laboratory. The events were therefore transformed into the two-photon rest frame to define the production angle θ^* appropriately. The data were then corrected, using fully simulated QED Monte Carlo events, to remove the effects of both residual radiative corrections and detector inefficiencies. The lowest order cross section was thus obtained, and is plotted in Fig. 2 together with the corresponding prediction. Though there is a two standard deviation deficit in the total number of events, the general shape of the distribution is consistent with QED expectations ($\chi^2/NDF = 23/19$).

At present integrated luminosities, statistical errors dominate over systematics in all comparisons of the data with models. The sources of systematic uncertainty listed in Table 2 are, however, taken into account in all fits to the data. The uncertainty in selection efficiency was assessed by varying cuts according to the experimental calibration uncertainties. The Monte Carlo contains contributions to order α^3 with both soft and hard photon emission. The effect of missing higher orders is estimated to be $< 0.6\%$ [19] by comparing α^3 corrections to the lowest order process. This was checked by measuring the number of four-photon events in the high statistics data recorded at the Z peak. Added in quadrature, the total systematic uncertainty is 1.5%, and this is treated as an uncertainty in the overall normalisation of the data.

| | |
|----------------------------|--------|
| Photon selection | 0.6% |
| Converted photon selection | 0.3% |
| Integrated luminosity | 0.9% |
| Monte Carlo statistical | 0.8% |
| Monte Carlo theoretical | < 0.6% |
| Total (in quadrature) | 1.5% |

Table 2: Systematic uncertainties in the two-photon analysis

4.2 Searches for Physics beyond the Standard Model

A deviation in the observed data from the predictions of quantum electrodynamics could be evidence for physics beyond the Standard Model, such as effects due to contact interactions or the exchange of an excited electron. Similarly, the lack of any observed deviation allows constraints to be placed on the parameters of models for new physics. A number of such models are considered below, all of which can be parameterised by the general equation

$$\frac{d\sigma}{d\Omega} = \left(\frac{d\sigma}{d\Omega} \right)_{\text{QED}} (1 + f(q^2, \epsilon)),$$

where f is some function of q^2 , the momentum transfer squared and ϵ , a parameter of the model depending on, for example, cut-off parameters or the mass of an excited electron. A fit was then performed of the experimental distribution in $\cos\theta$ to the prediction of each model, in order to determine the 95% confidence level limits on its parameter.

A log likelihood method was used to fit the data, with the likelihood function \mathcal{L} given by

$$\mathcal{L}(\epsilon, N) = \frac{1}{\sqrt{2\pi}\Delta N} \exp\left(-\frac{1}{2}\left(\frac{1-N}{\Delta N}\right)^2\right) \prod_{i=1}^{\text{nbins}} \mathcal{P}(\alpha_i, \eta_i(\epsilon, N)).$$

Here $\mathcal{P}(n, x)$ is the Poisson probability to observe n events from a distribution of mean x , α_i is the observed number of events in a bin of $\cos\theta$, and η_i is the model prediction. The relative normalisation, N , was allowed to vary from its expected value of 1 with a standard deviation of ΔN , corresponding to the overall systematic uncertainty of 1.5%.

Deviations from QED are usually characterised by cut-off parameters Λ_+ and Λ_- . The modified QED differential cross section is then generally expressed as

$$\frac{d\sigma}{d\Omega} = \left(\frac{d\sigma}{d\Omega} \right)_{\text{QED}} \left(1 \pm \frac{s^2}{2\Lambda_{\pm}^4} (1 - \cos^2\theta^*) \right).$$

The log likelihood fit was performed with respect to ϵ_{\pm} , defined as $\pm\Lambda_{\pm}^{-4}$, and N . The 95% confidence level upper limits were obtained for ϵ_{\pm} by normalising the probability to the integral over the physically allowed region of the parameters, *i.e.* $\epsilon_+ > 0$, $\epsilon_- < 0$. The equivalent 95% confidence level lower limits on Λ_{\pm} are given in Table 3, along with the fitted value of ϵ with its one standard-deviation error. Fig. 3 shows the ratio of the observed cross section to that predicted by QED, as a function of $\cos\theta^*$. Also indicated, as dotted lines, are the values which are obtained for a modified cross section given by the 95% confidence level limits on Λ_+ and Λ_- .

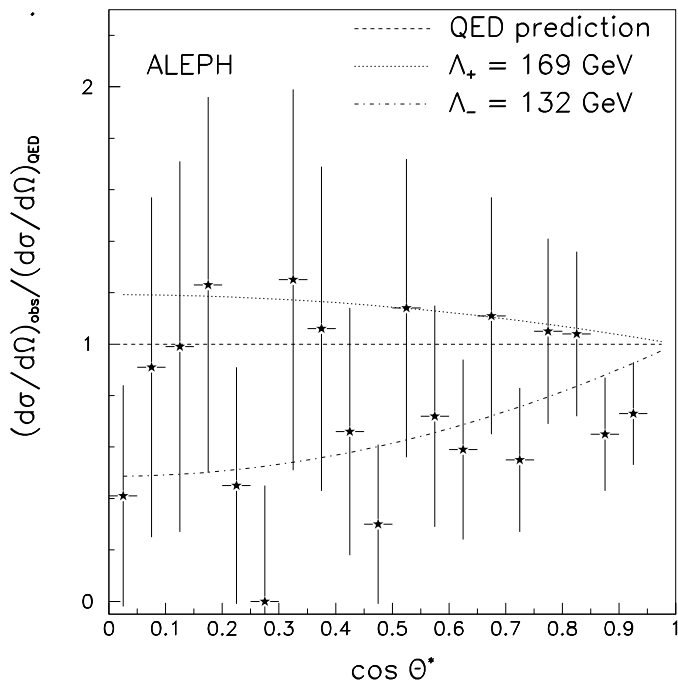


Figure 3: The ratio of the observed to predicted cross sections, for the process $e^+e^- \rightarrow \gamma\gamma(\gamma)$, as a function of $\cos \theta^*$. Also shown are the 95% confidence level limits on the QED cut-off model.

If two-electron, two-photon contact interactions exist, then the cross section for two-photon production becomes

$$\frac{d\sigma}{d\Omega} = \left(\frac{d\sigma}{d\Omega} \right)_{\text{QED}} + \left(\frac{d\sigma}{d\Omega} \right)_{\text{contact}},$$

where the second term includes both the contact interactions themselves and their interference term with QED (which is usually a larger effect). The exact form of the cross section depends on the chirality of the electron current that can take part in the interaction, leading to the possibility of left (L), right (R), L+R and L-R amplitudes. The expressions for the cross sections are given in [8] and [10].

A fit was performed in exactly the same way as for the simple QED cut-off model, with $\epsilon = \Lambda^{-4}$ except in the L-R case where the interference term vanishes and the lowest order dependence on Λ is Λ^{-8} . For this model, the fit was performed in Λ^{-8} , and the sensitivity is seen to be reduced. The results are shown in Table 3. An alternative description of extensions to QED is provided by considering non-standard effective Lagrangians containing operators of dimensions 6, 7 or 8 [20]. Making the same assumptions as the authors of Ref. [20] that $\Lambda = \tilde{\Lambda} \equiv \Lambda_6$, $\Lambda_S = \Lambda_P \equiv \Lambda_7$ and $\Lambda_A \equiv \Lambda_8$, the above procedure yields the following 95% confidence limits: $\Lambda_6 > 676$ GeV, $\Lambda_7 > 396$ GeV and $\Lambda_8 > 12.1$ GeV.

The reaction $e^+e^- \rightarrow \gamma\gamma$ can also proceed via the exchange of an excited electron. The cross section then depends on two parameters: the mass of the excited electron, M_{e^*} , and the $ee^*\gamma$ coupling. The simplest gauge-invariant form [21] of the interaction (the Low Lagrangian) leads to the differential cross section given in [22]. In this case, the fit was performed several times for different fixed values of M_{e^*} with $\epsilon = (\lambda/M_{e^*})^2$ being the variable parameter of the fit, and λ the

| Model | ϵ | Λ_+ (GeV) | Λ_- (GeV) |
|-------------|---|-------------------|-------------------|
| QED cut-off | $(-0.156 \pm 0.102) \times 10^{-8} \text{ GeV}^{-4}$ | 169 | 132 |
| L, R | $(-0.367 \pm 0.269) \times 10^{-8} \text{ GeV}^{-4}$ | 131 | 105 |
| L + R | $(-0.168 \pm 0.115) \times 10^{-8} \text{ GeV}^{-4}$ | 163 | 129 |
| L - R | $(-0.397 \pm 0.324) \times 10^{-16} \text{ GeV}^{-8}$ | 111 | — |

Table 3: Results for QED cut-off parameters and contact term interactions. The fitted parameter is given with its standard deviation, while the values for Λ_{\pm} are 95% confidence level lower limits.

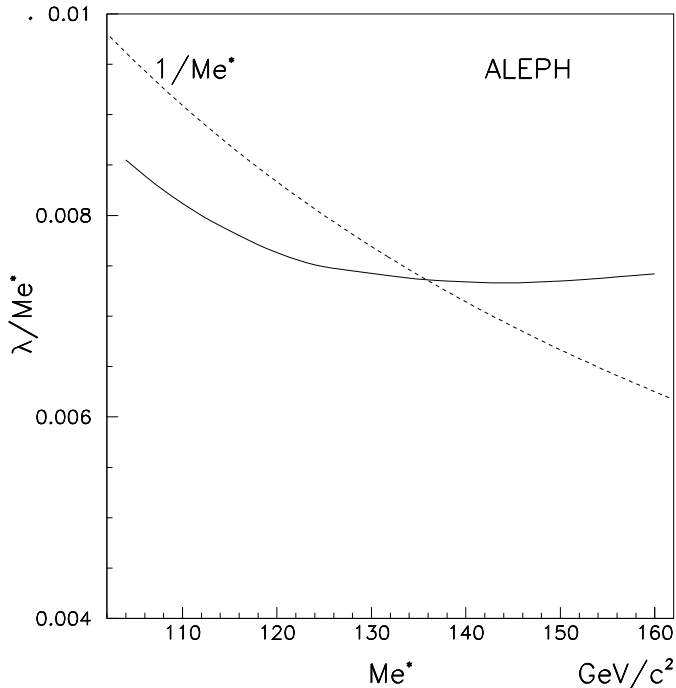


Figure 4: The 95% confidence level lower limit on (λ/M_{e^*}) (solid line) as a function of M_{e^*} . Also plotted (dotted line) is $1/M_{e^*}$, the intersection of the two lines giving the lower limit for the mass of the e^* if $\lambda = 1$.

ratio of the $ee\gamma$ to $ee^*\gamma$ couplings. The results are shown in Fig. 4, where the 95% confidence level upper limit on (λ/M_{e^*}) is plotted as a function of M_{e^*} . Also plotted is the value of $1/M_{e^*}$, and from the intersection point of the two lines it can be seen that the 95% confidence level lower limit on the mass of the excited electron is $136 \text{ GeV}/c^2$ if it is assumed that $\lambda = 1$. This result, and similar ones obtained by the OPAL [5] and L3 [9] collaborations, are however less constraining for the $ee^*\gamma$ coupling than those derived from analyses of the $ee\gamma$ final state [4, 23] for values of M_{e^*} up to almost the full centre-of-mass energy.

5 Conclusions

Single and multi-photon production has been studied in the ALEPH data collected during the 1995 high energy run of LEP. The cross sections for single, double and triple photon production were found to be compatible with the expectations of the Standard Model. No events were observed with four or more energetic photons.

The data from the two-photon analysis have been used to place limits on the parameters of a number of extensions to the Standard Model, notably the presence of $e^+e^-\gamma\gamma$ contact interactions and the exchange of a massive excited electron in the t channel. The 95% confidence level lower limits on the QED cut-off parameters Λ_+ and Λ_- were found to be 169 and 132 GeV, respectively. The effect of excited electron exchange depends on both the mass and coupling constant. In the simplest case, an assumption that the $ee^*\gamma$ coupling is equal to the $ee\gamma$ coupling yields a 95% confidence lower limit to M_{e^*} of 136 GeV/ c^2 . Contact term energy scale limits have also been obtained for the simplest extension to QED, with various allowed chiralities of the electron considered. In all cases, these limits obtained from the small amount of LEP high energy running are already competitive with the earlier published results obtained with larger integrated luminosities. The data from LEP II, where the energies and integrated luminosities will be higher still, are eagerly awaited.

Acknowledgements

We wish to congratulate our colleagues in the CERN accelerator divisions for their very successful operation of the LEP storage ring and for the impressive startup of the high energy run. We are grateful to the engineers and technicians in all our institutions for their contribution towards the excellent performance of ALEPH. Those of us from non-member countries thank CERN for its hospitality.

References

- [1] M. Chen et al., Phys. Rep. C159 (1988) 203;
R. Barbieri et al., CERN 89-08 Vol. 2 (1989) 121.
- [2] F. Boudjema and A. Djouadi, Phys. Lett. B240 (1990) 485.
- [3] ALEPH Collab., D. Decamp et al., Phys. Lett. B250 (1990) 172;
L3 Collab., B. Adeva et al., Phys. Lett. B252 (1990) 525;
OPAL Collab., M.Z. Akrawy et al., Z. Phys. C50 (1991) 373;
L3 Collab., O. Adriani et al., Phys. Lett. B275 (1992) 209;
L3 Collab., O. Adriani et al., Phys. Lett. B292 (1992) 463;
L3 Collab., O. Adriani et al., Phys. Lett. B297 (1992) 469;
ALEPH Collab., D. Buskulic et al., Phys. Lett. B313 (1993) 520;
L3 Collab., O. Adriani et al., Phys. Rep. 236 (1993) 1;
OPAL Collab., R. Akers et al., Z. Phys. C65 (1995) 47;
L3 Collab., M. Acciarri et al., Phys. Lett. B346 (1995) 190;
DELPHI Collab., P. Abreu et al., CERN PPE-96-03 submitted to Z. Phys.
- [4] L3 Collab., M. Acciarri et al., CERN PPE-95-190 submitted to Phys. Lett. B.
- [5] OPAL Collab., G. Alexander et al., CERN PPE-96-039 submitted to Phys. Lett. B.
- [6] L3 Collab., B. Adeva et al., Phys. Lett. B250 (1990) 199;
OPAL Collab., M.Z. Akrawy et al., Phys. Lett. B257 (1991) 531;
DELPHI Collab., P. Abreu et al., Phys. Lett. B268 (1991) 296;
L3 Collab., O. Adriani et al., Phys. Lett. B288 (1992) 404;
DELPHI Collab., P. Abreu et al., Phys. Lett. B327 (1994) 386;
L3 Collab., M. Acciarri et al., Phys. Lett. B353 (1995) 136.
- [7] ALEPH Collab., D. Decamp et al., Phys. Rep. 216 (1992) 253.
- [8] ALEPH Collab., D. Buskulic et al., Z. Phys. C59 (1993) 215.
- [9] L3 Collab., M. Acciarri et al., CERN PPE-96-048 submitted to Phys. Lett. B.
- [10] VENUS Collab., K. Abe et al., Z. Phys. C45 (1989) 175;
K. Hagiwara and K. Hikasa, KEK internal note (1988), unpublished.
- [11] P. Méry, M. Perrottet, F.M. Renard, Z. Phys. C38 (1988) 579;
F. Boudjema, F. Renard, Z Physics at LEP 1, CERN 89-08 Vol. 2 (1989) 1.
- [12] ALEPH Collab., D. Decamp et al., Nucl. Instrum. Methods A294 (1990) 121.
- [13] ALEPH Collab., D. Buskulic et al., Nucl. Instrum. Methods A360 (1995) 481.
- [14] R. Miquel, C. Mana and M. Martinez, Z. Phys. C48 (1990) 309.
- [15] S. Jadach, B.F.L. Ward and Z. Was, Comp. Phys. Commun. 79 (1994) 503.
- [16] F.A. Berends and R. Kleiss, Nucl. Phys. B186 (1981) 22.

- [17] P. Janot, Tests of QED to $O(\alpha^3)$ and $O(\alpha^4)$ and a search for excited leptons, using the CELLO detector at PETRA, PhD Thesis, LAL 87-31 (1987).
- [18] F.A. Berends, R. Kleiss, W. Hollik, Z. Phys. C33 (1987) 433.
- [19] E. Barberio, A study of the reaction $e^+e^- \rightarrow \gamma\gamma(\gamma)$ at the LEP storage ring with the ALEPH detector, Ph.D. Thesis, Siegen University (1993).
- [20] O.J.P. Eboli et al., Phys. Lett. B271 (1991) 274.
- [21] F.E. Low, Phys. Rev. Lett. 14 (1965) 238.
- [22] A. Litke, Experiments with electron-positron colliding beams, Ph.D. Thesis, Harvard Univ (1970).
- [23] ALEPH Collab., D. Buskulic et al., Search for Excited Leptons in ALEPH at 130-140 GeV, in preparation.